



Durian (*Durio zibethinus*) ripeness detection using thermal imaging with multivariate analysis

Maimunah Mohd Ali^a, Norhashila Hashim^{a,b,*}, Muhammad Ikmal Shahamshah^a

^a Department of Biological and Agricultural Engineering, Faculty of Engineering, Universiti Putra Malaysia, 43400 Serdang, Selangor, Malaysia

^b SMART Farming Technology Research Centre, Faculty of Engineering, Universiti Putra Malaysia, 43400 Serdang, Selangor, Malaysia

ARTICLE INFO

Keywords:

Durian
Thermal imaging
Multivariate analysis
Ripeness detection
Machine learning

ABSTRACT

The detection of durian ripeness using thermal imaging is an essential study geared towards improving the current analytical methods which rely heavily on routine analysis and human labour skills. Thermal imaging was investigated in this study in order to evaluate the ripeness of durian based on the relationship of physicochemical properties and thermal image parameters. Thermal images of durians were acquired at three different ripening stages (unripe, ripe, and overripe) and the physicochemical properties of the soluble solids content, pH, firmness, moisture content, and colour changes were determined. Partial least squares (PLS) regression was used to develop quantitative prediction models with R^2 values greater than 0.94 for all the physicochemical properties of durians. Principal component analysis (PCA) showed successful clustering ability of three different ripeness levels of durians. Linear discriminant analysis (LDA), k-nearest neighbour (kNN), and support vector machine (SVM) were applied for the establishment of the optimal classification modelling algorithms. The SVM classifier gave the overall best performance for the discrimination of durian ripeness with a classification accuracy of 97 %. The feasibility of thermal imaging coupled with multivariate methods demonstrated huge potential for non-destructive evaluation of durian ripeness levels.

1. Introduction

Durian (*Durio zibethinus*), a member of the Bombaceae family is an important economic crop in Southeast Asian countries, specifically in Thailand, Malaysia, Indonesia, and the Philippines (Voon et al., 2007). Malaysia has shown a rising trend in durian production over the last few years to sustain the supply and export demand with an estimated annual production of more than 300,000 million tonnes per year (DOA, 2019). It has recently gained market penetration in China which accounted for about \$600 million and the values are expected to increase by 50 % by 2030 (Teh et al., 2017). There are many durian cultivars which are very diverse in taste, aroma, texture, nutritional composition, flesh colour, as well as variations in the size and shape of the fruit. The fruit is exported in whole fruit form, either fresh or frozen at which the ripening stage of the fruit is of major criteria that hugely influences its quality. Several criteria are employed to detect the ripeness of durian, such as the sound that comes from tapping the durian husk, key volatile compounds, colour and elasticity of the spine, number of days after anthesis, etc. (Kuson and Terdwongworakul, 2013; Mohd Ali et al., 2020a). The most

popular approach is by allowing the fruit to ripen naturally on the trees with regard to obtaining maximum-quality flavour, aroma, texture, and appearance. In order to preserve the fruit quality, the durians that have fallen to the ground must be collected immediately to avoid contact with dirt and infection by pathogens (Voon et al., 2006). The collected durian is then transported to the wholesale market or packing house for export.

Durian has a tendency to split easily when it is harvested during the unripe stage (Siriphanich, 2011). On the other hand, overripe fruit tends to perish rapidly rendering it unsuitable for sale besides affecting consumer perception. Although several studies have been conducted to detect ripening stages in durian, the methods are mostly destructive such as determination of pulp dry weight and carotenoid content using routine analysis or minimally destructive in terms of loss of desirable texture due to the spiky surface of the fruit (Youryon et al., 2018). Even so, the destructive method may not be performed effectively due to the bulk volume of durian exports and limitations concerning skilled labour and experience (Phuangsoombut et al., 2018). Fruit quality evaluation without sample destruction and off-line interruption was a major challenge for durian growers and researchers (Onsawai and Sirisomboon,

* Corresponding author at: Department of Biological and Agricultural Engineering, Faculty of Engineering, Universiti Putra Malaysia, 43400, Serdang, Selangor, Malaysia.

E-mail address: norhashila@upm.edu.my (N. Hashim).

<https://doi.org/10.1016/j.postharvbio.2021.111517>

Received 21 October 2020; Received in revised form 18 February 2021; Accepted 19 February 2021

Available online 28 February 2021

0925-5214/© 2021 Elsevier B.V. All rights reserved.

2015). Due to the huge demand and high price, durian growers are tempted to harvest the fruit prior to the optimum physiological maturity is reached.

A number of non-destructive techniques have been investigated for detection of ripeness of durian fruit. Tantisopharak et al. (2016) studied the electromagnetic scattering parameters of durians in order to monitor their ripeness. The natural frequency changes in relation to the fruit maturity contributed to the difference of resonant frequencies for the discrimination of durian based on several ripeness levels. Furthermore, Pensiri and Visutsak (2018) classified the ripeness of durian using the watershed segmentation technique. In this case, durian images were converted into binary images using the edge detection method before performing image segmentation. The findings demonstrated a good classification accuracy of up to 94 % in the recognition of durian ripeness. In another approach, Phuangsoombut et al. (2018) determined the absorbance of two parts of durian (rind and flesh) based on the maturity of the fruit. An empirical formulation model was developed to predict the dry matter content of the rind and flesh of the durian. It was revealed that an empirical formulation could be used to minimise the absorbance impact of rind and flesh of the fruit. As such, a direct non-destructive measurement is required that can represent the fruit maturity without damaging the fruit, either minimally or involving the whole fruit.

Thermal imaging is an infrared detection method that determines the spatial energy emitted from the surface of a material. The spatial energy is converted by the imaging unit into a thermal map denoted as a thermogram (Mohd Ali et al., 2020b). Starting with thermal cameras that are implemented for defect detection, this technique has advanced rapidly in food processing industries (Mangus et al., 2016). The non-destructive nature of thermal imaging technique coupled with the rapid online usability are the key factors for the fast-growing demand of this technique in numerous fields. Thermal imaging may be utilised not only for defect sorting but feasibly for monitoring quality evaluation.

Due to this characteristic and function, thermal imaging has presented promising results in the determination of texture, maturity, bruising, defects, and colour evaluation of several fruit such as apples (Chandel et al., 2018), pears (Hahn et al., 2016), mangoes (Naik and Patel, 2017), guavas (Gonçalves et al., 2016), and green citrus (Gan et al., 2018). Badia-Melis et al. (2016) successfully predicted the surface temperature of apples with different packaging boxes; plastic and cardboard using thermal imaging technique. Kuzy et al. (2018) developed a thermal imaging system and explored its feasibility in detecting bruised blueberries non-destructively. In the same manner, Ding et al. (2017) developed classification abilities based on volatile compounds obtained from the thermal images of fresh, seriously decayed, and moderately decayed grapes with correct classification accuracies of 100 %, 93.3 %, and 90 %, respectively. Despite the importance of durian as an economic value crop with its distinctive strong smell, a fundamental study of the thermal imaging approach for this application is almost non-existent. With the advent of optical technology, there is a potential to enhance the application of thermal imaging by adopting advanced multivariate tools. The thermal imaging technique was utilised in order to detect the durian ripeness by employing multivariate algorithms as a fast and non-destructive assessment tool. Thus, this study aims to evaluate the quality evaluation of durian based on different ripeness levels using thermal parameter data combined with multivariate algorithms.

2. Material and methods

2.1. Fruit samples

Durians of the 'Durian Kampung' (888) variety were obtained from the Durian Nursery, Taman Pertanian Universiti, Universiti Putra Malaysia. The durian samples were randomly selected and divided into three groups at the chronological stages of 108 (unripe), 125 (ripe), and 138 (overripe) days after anthesis. A total of 90 durian samples comprising of 30 fruit at each ripeness level were obtained and

transported immediately to the laboratory in which the fruit were acclimatised for 24 h at a controlled temperature of 25 °C and relative humidity of 85 %. The samples were cleaned and weighed before conducting the image acquisition process.

2.2. Thermal imaging acquisition

An infrared thermal camera (FLIR E60, FLIR systems, King Hills, United Kingdom) ranging from 700 nm until 1400 nm, temperature ranging from −20 °C to +650 °C equipped with a resolution 320 × 240 pixels and thermal sensitivity less than 0.05 °C was utilised to obtain thermal images of the durian samples. The emissivity coefficient of durians was determined to be equalled to 0.94 using the method provided by Doosti-Irani et al. (2016). Calibration check for thermal imaging was conducted by measuring targets or durian samples with known temperatures to make a baseline measurement prior to image acquisition. The thermal imaging device was calibrated with a black-body reference source which could absorb and radiate electromagnetic radiation. The emissivity related to the fruit sample was used to be stored in the imaging programme in an attempt to accurately detect the radiation emission. Thermal images were captured at a fixed distance of 40 cm from the sample. A total of 270 thermal images were acquired for the overall durian samples. The image acquisition was performed at ambient temperature for the detection of durian ripeness. The raw and thermal images of durians at different ripeness levels are shown in Fig. 1.

2.3. Reference methods

2.3.1. Colour evaluation

The instrumental colour readings were obtained from a colorimeter (NR20XE, Shenzhen 3 nh Technology Ltd., China). The colour readings of the durian pulps were measured in three measurements of each sample. The mean of these measurements was determined and the colour description of the fruit was described as CIE values for lightness (L^*), redness (a^*), yellowness (b^*), chroma (C^*), and hue (H^*).

2.3.2. Firmness

The firmness of the durian pulp was measured using an electronic fruit penetrometer fitted with a 5.0 mm diameter plunger tip (GY-1, G-tech Ltd., China). The plunger was inserted to a depth of 0.5 cm and the maximum force values were recorded. The average values of the firmness readings were expressed in Newton (N).

2.3.3. Soluble solids content

The soluble solids content was examined according to Voon et al. (2006) by using a refractometer (Pal-1, Atago Co., Tokyo, Japan). The durian pulp was blended and filtered through muslin cloth before performing the SSC measurements. The SSC results were expressed as %.

2.3.4. pH

The pH of the pulp was measured using a pH meter (DPH-2, Atago Co., Tokyo, Japan). The calibration was done prior to measurement using a buffer pH 7.0 solution.

2.3.5. Moisture content

The measurement of the moisture content was performed by taking the durian pulp from the middle part of every locule. The fruit was cut into several pieces and approximately 20 g of the mixed pulp sample was dried in a hot air oven at 70 °C for 24 h.

2.4. Thermal image processing

The thermal images of durian fruit at three different ripeness levels were examined using Matlab software (Version R2020a, The Math-Works, USA). The thermal images of the durian samples were converted to grayscale images. The mean pixel value of each thermal image was

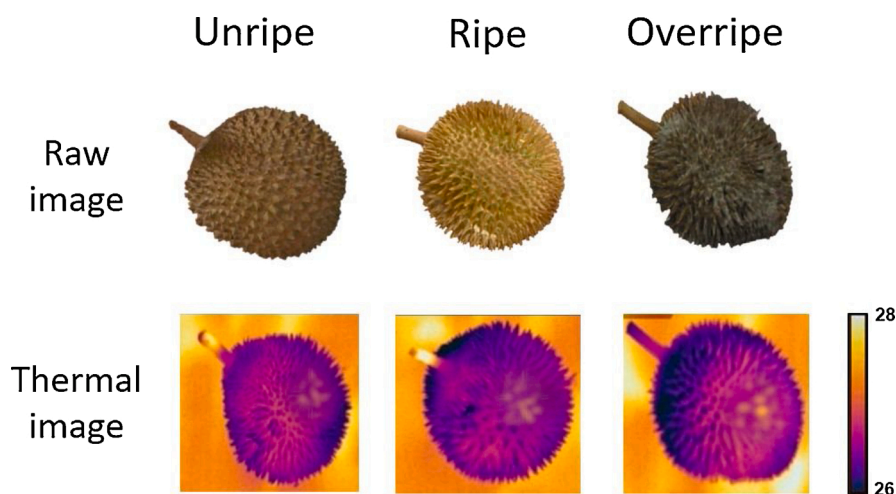


Fig. 1. The raw and thermal images of durians at different ripeness levels. The colours in the thermal colour bar corresponded to the temperature difference of different group of ripeness levels within the range of 26–28 °C.

determined by selecting a region of interest (ROI) to eliminate the noise in the background image. The ROI was segmented using a thresholding technique where the optimal threshold value was calculated to separate the background from the thermal image. After extracting the ROI, the thermal image was converted to a binary image. In order to enhance the quality of an image, the binary image was then converted to grayscale image using Gaussian filter. The feature extraction from the thermal images was obtained from the segmented images based on the pixel values known as thermal parameters. To establish a correlation between quality attributes and thermal parameters of durians, the calculation of feature values was determined based on the pixel value and shape measurements. Using the properties of image regions, six features were selected based on the pixel value measurement. The selected thermal parameters were maximum intensity, minimum intensity, average intensity, mean of ROI (mean_ROI), maximum of ROI (max_ROI), and minimum of ROI (min_ROI). The maximum intensity, minimum intensity, and average intensity were retrieved from the pixel intensity based on the shape measurement of the image. Meanwhile, the mean_ROI, max_ROI, and min_ROI were obtained from the pixel values extracted from the ROI. All the thermal parameters were derived from the remarkable parts of the thermal image as a compact feature vector.

2.5. Multivariate data analysis

Descriptive statistics were calculated to provide a quantitative analysis of the data. Analysis of variance (ANOVA) was analysed to determine the significant differences between the durian samples and ripeness levels. The mean values between the quality attributes of durian at different ripeness levels were compared using Tukey's HSD test. Both descriptive statistics and ANOVA were performed using SAS software (Version 9.4, SAS Institute, Cary, NC, USA). The whole dataset was randomly split into calibration (70 %) and cross-validation (30 %) sets, respectively. Principal component analysis (PCA) was employed to evaluate the classification representation between the ripeness levels of the durians. The thermal images from the calibration set were used to visualise the distribution of the ripeness levels of the fruit. Two principal components (PC), namely PC1 and PC2 were used from the greatest contribution of total variance in order to identify the classification of durian ripeness. PCA loading was used to select the optimum thermal parameters for the prediction of quality attributes in durians.

Subsequently, a partial least squares (PLS) calculation was employed to predict the independent set of the samples. The PLS calibration models for predicting quality attributes of durians were obtained by cross-validation on the calibration datasets ($n = 180$) signifying 70 % of

the whole datasets ($n = 270$). On the other hand, cross-validation models were achieved with the remaining 30 % datasets ($n = 90$). A single ten-fold cross-validation was developed on the calibration set to select the optimal number of latent variables (LV) and error estimation of the PLS models. The goodness of fit and predictive capability of the PLS models was calculated based on the root mean squared error (RMSE) and coefficient of determination (R^2) between the measured and predicted values of the physicochemical properties of durians. Linear discriminant analysis (LDA), k-nearest neighbour (kNN), and support vector machine (SVM) algorithms are different multivariate tools that can be used to classify the ripeness of durian based on the thermal parameters (Fig. 2).

In addition, kNN was carried out to discriminate the ripeness groups from the training datasets by calculating the distance between the unknown sample and the number of nearest neighbours. The optimum k-value (constant) was selected from the highest classification accuracies during the implementation of the kNN algorithm. The k-value was

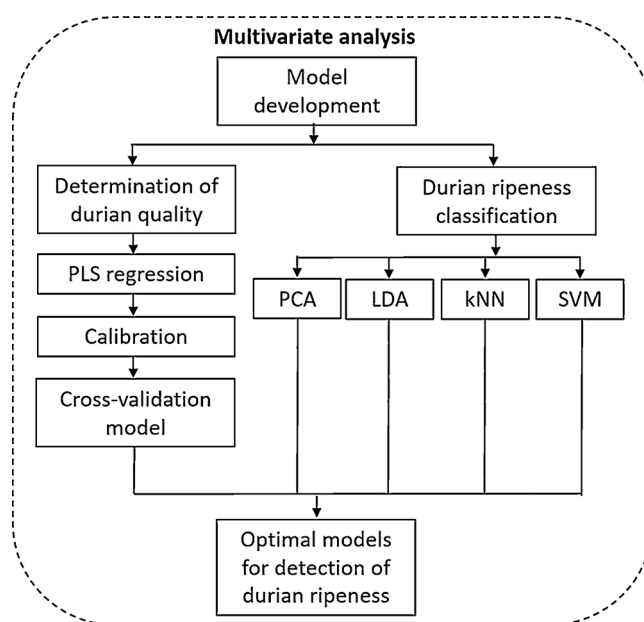


Fig. 2. Procedures for the detection of durian ripeness using thermal imaging system. PLS = partial least squares; PCA = principal component analysis; LDA = linear discriminant analysis; kNN = k-nearest neighbour; SVM = support vector machine.

optimised from 3 to 15 with a step of 1 using ten-fold cross-validation in order to train the classification algorithms. On the other hand, SVM is a binary classifier algorithm in which the optimal value of parameters was used to find the classification with the highest accuracy. By using the SVM algorithm, 30 % of the whole datasets were chosen as testing data, whereas the remaining data was considered as training datasets. Radial basis function was applied as the kernel parameters for the SVM models with the penalty coefficient value fixed to 1. All multivariate tools were developed in the Unscrambler X software (Version 10.3, CAMO Software, Oslo, Norway).

3. Results and discussion

3.1. Analysis of physicochemical properties

The quality attributes of durians at three different ripeness levels are shown in Table 1. A significant difference ($p < 0.05$) was obtained for all quality attributes of durians between the different ripeness levels. The SSC of the durians ranged from 19.63 % to 25.15 %, in which the highest value was recorded from the ripe group. These SSC values were in agreement with those investigated by Belgis et al. (2016) which were between 12.5 % and 23.0 %. Meanwhile, the effect of freezing and different thawing conditions on durian pulp reported SSC values ranged from 14.0 % to 24.4 % (Tagubase et al., 2016). It was noted that the ripe group had the highest SSC, signifying that durian ripeness was governed by the increase in sugar content during the ripening process of the fruit (Voon et al., 2007). The moisture content of durians steadily increased from unripe (62.76 %), followed by ripe (65.08 %) and overripe (67.18 %) groups, respectively. A similar finding was obtained for the determination of moisture content ranging from 56 to 69 % per 100 g fresh weight (FW) of durian pulp (Aziz and Jalil, 2019). For this reason, high moisture content in durians could also influence the texture and flavour of the fruit.

On the other hand, the firmness value gradually decreased from unripe (37.33 N) to overripe (10.42 N) groups, respectively. In order to describe the fruit firmness, Munera et al. (2017) reported that the firmness threshold below 18 N was defined as an indication of soft texture which would be susceptible to bruising or defects. This finding was also comparable to the texture softening observed where the firmness of durian pulp decreased along with the ripeness group from unripe to overripe (Wisutiamonkul et al., 2015). A similar decreasing trend was demonstrated for the pH of durian from unripe to overripe groups ranged from 7.22 to 5.82.

The colour changes of durian pulp varied for all colour parameters (L^* , a^* , b^* , C^* , and H^*). All colour properties of the durian samples varied significantly ($P < 0.05$) throughout the ripeness levels. A decline in a^* value was attained from 1.97 to 1.80 for unripe and ripe groups, respectively. However, the a^* value increased (3.99) for the overripe group. Likewise, the b^* and C^* values decreased from unripe to ripe

groups before slightly increasing in the overripe groups. This variation could be due to the different ripeness levels of durians upon processing, accounting to the inconsistency of pulp colour that was associated with the degradation of beta-carotene. The L^* value gradually decreased from unripe (86.85), followed by ripe (80.66) and overripe (74.35) groups. In a similar vein, these observations were also comparable with the $L^*a^*b^*$ colour values in fruit ranging from 6.46 to 68.13 (Sunilkumar and Sparjan Babu, 2013). The reduction in L^* value could also be explained by the possible reaction that occurred during the enzymatic activity and degradation of the fruit (Tagubase et al., 2016). In a similar manner, the H^* value decreased significantly for all ripeness levels ranging from 86.25 to 81.79 with the lowest value recorded by the overripe group. This result was in agreement with that reported by Tifani et al. (2018) in which the decline in H^* value might be linked to the high oxidised polyphenol content.

3.2. Changes of thermal parameters

The thermal parameters were selected based on the feature extraction of durian images to develop calibration and cross-validation models for the detection of ripeness levels of the fruit. The ANOVA results showed the means of thermal parameters of durians; maximum intensity, minimum intensity, average intensity, mean_ROI, max_ROI, and min_ROI between three different ripeness levels as presented in Table 2. All thermal parameters were highly influenced by ripeness levels at $P < 0.05$. The variation of thermal parameters described the distribution of pixel values of durians at different ripeness levels which were observed on the fruit surfaces. The results revealed that high dependency of thermal parameters at different ripeness levels indicated that these parameters were feasible to represent the behaviour of thermal images of durians.

The variation in terms of pixel intensities could be elucidated by the synthesis of the colour pigmentation in durian to be used for the classification of ripeness levels. It is important to establish fixed measuring distance during image acquisition in order to avoid interference and several environmental factors such as thermal reflection and ambient temperature (Izquierdo et al., 2020). The highest means achieved for minimum intensity (0.51), average intensity (0.64), and min_ROI (0.51) were significantly influenced by the unripe group, respectively. The max_ROI parameter (0.97) was found to be influenced by the ripe group. On the other hand, the thermal parameters that were greatly influenced within the overripe group were maximum intensity (0.96) and mean_ROI (0.68), respectively. In general, it was described that the behaviour of the thermal parameters was significantly influenced by the changes in pixel intensity among the ripeness levels of durian.

The information regarding the fruit estimation was collected based on the feature extraction of the thermal images (Sumriddetchkajorn and Intaravanne, 2013). The investigation performed by Doosti-Irani et al. (2016) proved that the multiple regression model was feasible to be used in the detection of bruise depth in apples based on the thermal maps and surface temperature of the fruit. A recent study by Zeng et al. (2020) suggested that the grey-level co-occurrence matrix of the thermal images were feasible in the bruise detection of pears. In another approach, Farokhzad et al. (2020) determined the optimum thermography conditions using the median, minimum, maximum, and mean values of thermal images for the detection of fungal infection of potato tubers at different heating and cooling treatments. These findings were in agreement with Naik and Patel (2017) who defined thermal parameters consisted of area, weight, and eccentricity based on size feature extraction for maturity grading of mangoes.

3.3. Prediction performance of durian quality

The PLS models were used to monitor the prediction of the quality attributes of durian based on the optimum thermal parameter measurement. The performance of calibration and cross-validation models

Table 1
Quality attributes of durian at three different ripeness levels.

Physicochemical properties	Ripeness level		
	Unripe	Ripe	Overripe
Soluble solids content (%)	19.63 \pm 4.31 ^a	25.15 \pm 6.42 ^{bc}	23.57 \pm 5.14 ^c
Moisture content (%)	62.76 \pm 5.93 ^a	65.08 \pm 4.54 ^{bc}	67.18 \pm 5.34 ^c
Firmness (N)	37.33 \pm 3.27 ^a	27.34 \pm 0.42 ^{bc}	10.42 \pm 0.01 ^c
pH	7.22 \pm 0.18 ^a	6.28 \pm 0.42 ^{bc}	5.82 \pm 0.40 ^c
L^*	86.85 \pm 4.14 ^b	80.66 \pm 6.79 ^{bc}	74.35 \pm 5.89 ^c
a^*	1.97 \pm 1.39 ^a	1.80 \pm 1.41 ^{bc}	3.99 \pm 1.62 ^c
b^*	28.59 \pm 4.43 ^a	26.75 \pm 5.16 ^{bc}	27.81 \pm 4.98 ^c
C^*	28.65 \pm 4.48 ^a	26.84 \pm 5.21 ^{bc}	28.14 \pm 5.01 ^c
H^*	86.25 \pm 2.49 ^a	86.36 \pm 2.63 ^{bc}	81.79 \pm 3.23 ^c

Data is expressed as a mean with three replicates (\pm standard error). Different letters indicate significantly difference ($P < 0.05$) by Tukey's HSD test within the same row.

Table 2

Thermal parameters based on durian feature extraction at three ripeness levels. The thermal parameters used are defined as: mean_ROI = mean of region of interest; max_ROI = maximum of region of interest; min_ROI = minimum of region of interest.

Ripeness level	Maximum intensity	Minimum intensity	Average intensity	mean_ROI	max_ROI	min_ROI
Unripe	0.94 ± 0.03 ^a	0.51 ± 0.02 ^a	0.64 ± 0.04 ^a	0.65 ± 0.03 ^a	0.95 ± 0.01 ^a	0.51 ± 0.02 ^a
Ripe	0.95 ± 0.01 ^{bc}	0.48 ± 0.02 ^{bc}	0.62 ± 0.06 ^{bc}	0.66 ± 0.03 ^{bc}	0.97 ± 0.01 ^{bc}	0.48 ± 0.02 ^{bc}
Over ripe	0.96 ± 0.01 ^c	0.49 ± 0.01 ^c	0.58 ± 0.04 ^c	0.68 ± 0.01 ^c	0.96 ± 0.01 ^c	0.49 ± 0.01 ^c

Data is expressed as mean with three replicates (± standard error). Different letters indicate significantly different ($P < 0.05$) by Tukey's HSD test within the same column.

of the physicochemical properties of durian using thermal imaging system is tabulated in Table 3. The PLS statistical indicators consisting of the R_c^2 and RMSEC for calibration as well as R_{cv}^2 and RMSECV for cross-validation were calculated to determine the predictive performance of the quality attributes of durian by means of a thermal imaging system. For the moisture content and firmness, both quality attributes recorded similar predictive performance with R_c^2 of 0.997 and R_{cv}^2 of 0.998, respectively. Moisture content and firmness were the most common quality attributes where these parameters were found to be superior to demonstrate the robustness of the imaging system, especially for detecting fruit maturation (Somton et al., 2015). The performance based on R^2 for the validation of moisture content in durian was also evaluated in the work by Phuangsoombut et al. (2018) who observed the ability of PLS models in the application of near-infrared spectroscopy with a predictive performance higher than 0.85. The predictive ability of the PLS model was significantly improved which signified that the calibration ($R_c^2 = 0.998$, RMSEC = 0.054) and cross-validation ($R_{cv}^2 = 0.999$, RMSECV = 0.088) models could demonstrate good prediction of SSC in durian fruit. On the other hand, prediction results of pH also showed good predictive values with an R_c^2 of 0.943 and R_{cv}^2 of 0.966, respectively. In this sense, the optimum thermal parameters for those quality attributes were found to be of average intensity. To establish a real-time imaging system for the detection of durian ripeness, this result helped to identify the optimum thermal parameters for the prediction of the physicochemical properties of the fruit.

With regard to the colour parameters, the calibration models obtained the values for L^* ($R_c^2 = 0.975$, RMSEC = 0.521), a^* ($R_c^2 = 0.984$, RMSEC = 0.218), and b^* ($R_c^2 = 0.968$, RMSEC = 0.195), respectively. On the contrary, the cross-validation models achieved the values for L^* ($R_{cv}^2 = 0.985$, RMSECV = 0.015), a^* ($R_{cv}^2 = 0.989$,

RMSECV = 0.196), and b^* ($R_{cv}^2 = 0.975$, RMSECV = 0.066), respectively. The PLS models also showed better predictive performances for the C^* parameter with an R_c^2 of 0.995 and R_{cv}^2 of 0.999. A similar trend was observed for the H^* parameter which exhibited excellent predictive performance with an R_c^2 of 0.947 and R_{cv}^2 of 0.969, respectively. In brief, carotenoids and anthocyanins are responsible for the visual appearances and colour distribution in fruit (Timkhum and Terdwong-worakul, 2012). For this purpose, more than one colour parameter was recommended for the assessment of fruit ripeness since the discrimination of ripeness stages could be incorporated for the prediction and classification tasks (Li et al., 2018). Intuitively, the variation of colour parameters denoted that the ripeness of each fruit possessed a diverse distribution that could be used to distinguish different types of fruit (Munera et al., 2017). As for the optimum thermal parameters for the colour evaluation of durian, the min ROI parameter was found to be the best parameter performance to represent the consideration of the computational prediction of the regression models.

The application of thermal imaging in determining the quality attributes of fruit was reported in various works such as bruise detection (Kuzu et al., 2018), fungal identification (Farokhzad et al., 2020), ripeness detection (Jawale and Deshmukh, 2017), etc. In addition, Zeng et al. (2020) examined the feasibility of thermal imaging ranging from a wavelength region of 8000–14000 nm for bruise identification of pears. The thermal images of bruised and non-bruised pears demonstrated changes in the cooling rate of fruit at a controllable temperature. Multivariate analysis techniques employed that thermal imaging can be characterised into qualitative classification and quantitative regression. The implementation of multivariate analysis with thermal imaging is recommended to increase the classification rate as well as improve the accuracy of fruit detection. With the purpose of development of real-time durian ripeness detection, the number of LVs was optimised in order to determine the optimal thermal parameters. The selected thermal parameters were used in the PLS model to validate the ripeness detection of durian with respect to each quality attribute of the fruit.

3.4. Comparison of classification models

It was found that the thermal images with average temperatures between 26 and 28 °C signified the most significant difference in relation to the ripeness detection of the fruit. The thermal images of different groups of ripeness levels obtained a temperature difference of 2 °C. Moreover, it was observed that the temperature recorded for thermal images of durians were the lowest at overripe level (26 °C) and the highest at the unripe level (28 °C). The slight difference in terms of temperature was normalised between 0 and 1 in order to achieve a reasonable contrast ability. The analysis of thermal images based on the feature extraction attributed to the temperature differences among the maturity stages which may be well-suited during data processing (Zeng et al., 2020). Additionally, it is necessary to consider a wide range of experimental conditions during the development of predictive models considering the variation in fruit maturity (Izquierdo et al., 2020).

The PCA model was used to determine the clustering capability at the three different ripeness levels, namely unripe, ripe and overripe durians. According to the corresponding PCA score plot, it can be described that the three ripeness levels of durian were discriminated successfully by two principal components (PC), which were PC1 (1 %) and PC2 (99 %)

Table 3

The performance of partial least squares (PLS) models for the determination of quality attributes in durian using thermal imaging system.

Parameter	LVs	Calibration		Cross-validation		Optimum thermal parameter
		R_c^2	RMSEC (%)	R_{cv}^2	RMSECV (%)	
Soluble solids content (%)	6	0.998	0.054	0.999	0.088	average intensity
Moisture content (%)	6	0.997	0.063	0.998	0.007	average intensity
Firmness (N)	6	0.997	0.056	0.998	0.095	average intensity
pH	6	0.943	0.426	0.966	0.252	average intensity
L^*	6	0.975	0.521	0.985	0.015	min_ROI
a^*	6	0.984	0.218	0.989	0.196	min_ROI
b^*	6	0.968	0.195	0.975	0.066	min_ROI
C^*	6	0.995	0.063	0.999	0.017	min_ROI
H^*	6	0.947	0.142	0.969	0.109	min_ROI

LV: Latent variables; R^2 : Coefficient of determination; RMSEC: Root mean square error of calibration; RMSECV: Root mean square error of cross-validation; min_ROI: minimum of region of interest.

based on the thermal parameters, collecting a total variance of 100 % (Fig. 3). With regard to the clustering scores associated with the durian ripeness and the location of the thermal parameters, the correlation loadings were well correlated with the respective PCs which explained 82 % of the variance (26 % and 56 %), respectively. The loading analysis assisted in the identification of the important thermal parameters responsible for the discrimination of the ripeness level of the durians. From the results, average intensity, minimum intensity, mean ROI, and min ROI could be an important parameter for the detection of durian ripeness in order to describe the effect of postharvest maturation based on the exterior ellipse in the plot. The PCA results demonstrated that the thermal parameters could discriminate durian according to the respective ripeness levels, namely unripe, ripe, and overripe. All durian samples comprising three ripeness levels were organised in homogenous clusters, signifying that different durian ripeness could be clearly classified by PCA based on the thermal parameters.

Based on the thermal parameters obtained from the feature selection, the classification accuracy of the models was improved with a larger

total number of features. However, the correct classification rates would also decline due to overfitting when the features increased. In this case, several multivariate algorithms were chosen to select the most suitable classifier for the classification task in the detection of durian ripeness. Regarding the discrepancy in the classification rates between the ripeness levels, it is vital to consider the quality evaluation of durian which demonstrated reliable results in the whole classification tasks. The average classification accuracies of durian at different ripeness levels using three multivariate algorithms (LDA, kNN, and SVM) are tabulated in Table 4. For the unripe group, the SVM models achieved the highest correct classification of 97 % followed by LDA (96 %) and kNN (95 %) models, respectively. Likewise, similar findings were obtained by SVM models with the highest classification accuracy of 96 % and 99 % for the ripe and unripe groups, respectively. In comparison of the three different multivariate algorithms, the SVM model showed the best overall classification performance (97 %), followed by LDA (96 %), and kNN (95 %) models. It can be seen that the performance of all classifiers revealed high classification accuracies which is feasible to be used in the

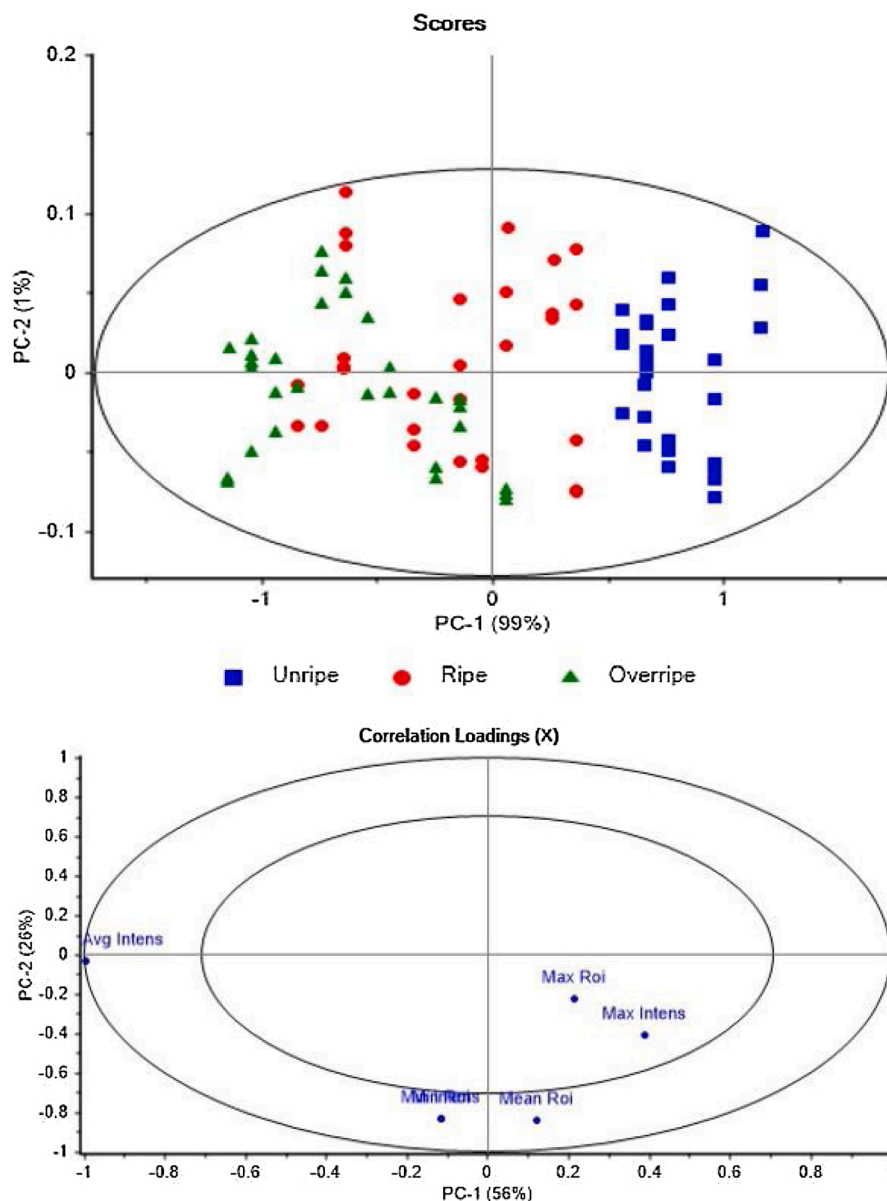


Fig. 3. The principal component analysis (PCA) score plots based on thermal parameters of three different ripeness levels of durians. The thermal parameters are defined as: Max Intens = maximum intensity; Min Intens = minimum intensity; Avg Intens = average intensity; Mean Roi = mean of region of interest; Max Roi = maximum of region of interest; Min ROI = minimum of region of interest.

Table 4

The average classification accuracies of durian at different ripeness levels using various multivariate algorithms.

Ripeness level	Correct classification (%)		
	LDA	kNN	SVM
Unripe	96	95	97
Ripe	95	93	96
Overripe	96	96	99
Overall	96	95	97

Multivariate algorithms used: LDA = linear discriminant analysis; kNN = k-nearest neighbour; SVM = support vector machine.

discrimination of ripeness levels of durian using a thermal imaging system.

Based on the findings, it can be noted that the SVM algorithm could classify the fruit into three commercial ripeness levels with high accuracy, which is simpler than high dimensional multiple regression analysis. Likewise, the SVM algorithm was found to be feasible for fruit classification according to the different ripening stages retrieved from the shape and texture features with the least error values for the classification accuracy (Azarmdel et al., 2020). In addition, Kuzy et al. (2018) investigated that LDA and SVM classifiers were both had strong classification performances in order to discriminate the bruise detection of blueberries. Similar results were achieved by Timkhun and Terdwongworakul (2012) who obtained good classification rates up to 94 % using PLS-DA model to classify durian maturity classes ranging from 113 to 134 days after anthesis. Raza et al. (2015) classified fungal contamination in tomatoes using the local feature set from thermal images using the SVM method. High accuracy of up to 90 % was identified by the SVM method for the detection of tomatoes infected with *Oidium neolyopersici*. Since the conventional method of durian ripeness detection restricts the practical application of fruit sorting after harvest, it is worthwhile to mention that the classification models can be successfully applied to overcome this problem. Regardless of the multivariate algorithms and the datasets, the performance of thermal imaging was found suitable for durian ripeness detection. Considering different ripeness levels of the fruit, thermal imaging coupled with multivariate algorithms showed strong ability for the classification purpose.

4. Conclusion

This study demonstrates the feasibility of thermal imaging to evaluate the ripeness detection of durian at three different ripeness levels. Among the thermal parameters obtained from the feature extraction methods, average intensity and min_ROI were chosen as the optimal parameters to distinguish durian fruit into unripe, ripe, and overripe groups. The PLS models yielded good prediction of all physicochemical properties of durians with $R^2 > 0.94$. On the other hand, the ripening evolution of the fruit could be observed through the PCA model in a non-supervised manner which provided mapping of the selected thermal parameters. The LDA, kNN, and SVM models were built to discriminate durian fruit according to three ripeness groups. By comparing the performance of the three multivariate tools, the highest performance was obtained by the SVM model with the overall accuracies of 97 % for durian ripeness detection. These classification models described the configuration of a thermal imaging system which provided a realistic scenario for the detection of durian ripeness. The development of thermal imaging coupled with multivariate analysis contributes to the advance of non-invasive techniques for quality evaluation of durian. The promising results create an opportunity and alternative method to adopt the multivariate models that deliver rapid and objective measurements.

CRediT authorship contribution statement

Maimunah Mohd Ali: Data curation, Visualization, Software,

Writing - original draft. Norhashila Hashim: Supervision, Conceptualization, Writing - review & editing. Muhammad Ikmal Shahamshah: Investigation, Data curation, Methodology, Formal analysis.

Declaration of Competing Interest

The authors report no declarations of interest.

Acknowledgements

The authors are thankful for the support and facilities provided by the Department of Biological and Agricultural Engineering, Faculty of Engineering, Universiti Putra Malaysia.

References

- Azarmdel, H., Jahanbakhshi, A., Mohtasebi, S.S., Muñoz, A.R., 2020. Evaluation of image processing technique as an expert system in mulberry fruit grading based on ripeness level using artificial neural networks (ANNs) and support vector machine (SVM). *Postharvest Biol. Technol.* 166, 1–12. <https://doi.org/10.1016/j.postharvbio.2020.111201>.
- Aziz, N.A.A., Jilil, A.M.M., 2019. Bioactive compounds, nutritional value, and potential health benefits of indigenous durian (*Durio Zibethinus* Murr.): a review. *Foods* 8, 1–18. <https://doi.org/10.3390/foods8030096>.
- Badia-Melis, R., Qian, J.P., Fan, B.L., Hoyos-Echevarria, P., Ruiz-García, L., Yang, X.T., 2016. Artificial neural networks and thermal image for temperature prediction in apples. *Food Bioprocess Technol.* 9, 1089–1099. <https://doi.org/10.1007/s11947-016-1700-7>.
- Belgis, M., Wijaya, C.H., Apriyanton, A., Kusiantoro, B., Yuliana, N.D., 2016. Physicochemical differences and sensory profiling of six lai (*Durio kutejensis*) and four durian (*Durio zibethinus*) cultivars indigenous Indonesia. *Int. Food Res. J.* 23, 1466–1473.
- Chandel, A.K., Khot, L.R., Osroosh, Y., Peters, T.R., 2018. Thermal-RGB imager derived in-field apple surface temperature estimates for sunburn management. *Agric. For. Meteorol.* 253–254, 132–140. <https://doi.org/10.1016/j.agrformet.2018.02.013>.
- Ding, L., Dong, D., Jiao, L., Zheng, W., 2017. Potential using of infrared thermal imaging to detect volatile compounds released from decayed grapes. *PLoS One* 12, 1–11. <https://doi.org/10.1371/journal.pone.0180649>.
- DOA, 2019. Statistik Tanaman (Sub-sektor Tanaman Makanan) 2019. Retrieved from. http://www.doa.gov.my/index/resources/aktiviti_sumber/sumber_awan/maklumat_pertanian/perangkaan_tanaman/booklet_statistik_tanaman_2019.pdf.
- Doosti-Irani, O., Gollzarian, M.R., Aghkhani, M.H., Sadriani, H., Doosti-Irani, M., 2016. Development of multiple regression model to estimate the apple's bruise depth using thermal maps. *Postharvest Biol. Technol.* 116, 75–79. <https://doi.org/10.1016/j.postharvbio.2015.12.024>.
- Farokhzad, S., Modares Motlagh, A., Ahmadi Moghadam, P., Jalali Honarmand, S., Kheiralipour, K., 2020. Application of infrared thermal imaging technique and discriminant analysis methods for non-destructive identification of fungal infection of potato tubers. *J. Food Meas. Charact.* 14, 1–7. <https://doi.org/10.1007/s11694-019-00270-w>.
- Gan, H., Lee, W.S., Alchanatis, V., Ehsani, R., Schueller, J.K., 2018. Immature green citrus fruit detection using color and thermal images. *Comput. Electron. Agric.* 152, 117–125. <https://doi.org/10.1016/j.compag.2018.07.011>.
- Gonçalves, B.J., de O. Giarola, T.M., Pereira, D.F., Boas, Vilas, de, E.V., B. de Resende, J. V., 2016. Using infrared thermography to evaluate the injuries of cold-stored guava. *J. Food Sci. Technol.* 53, 1063–1070. <https://doi.org/10.1007/s13197-015-2141-4>.
- Hahn, F., Cruz, J., Barrientos, A., Perez, R., Valle, S., 2016. Optimal pressure and temperature parameters for prickly pear cauterization and infrared imaging detection for proper sealing. *J. Food Eng.* 191, 131–138. <https://doi.org/10.1016/j.jfoodeng.2016.07.013>.
- Izquierdo, M., Lastra-Mejías, M., González-Flores, E., Cancellia, J.C., Aroca-Santos, R., Torrecilla, J.S., 2020. Deep thermal imaging to compute the adulteration state of extra virgin olive oil. *Comput. Electron. Agric.* 171, 105290. <https://doi.org/10.1016/j.compag.2020.105290>.
- Jawale, D., Deshmukh, M., 2017. Real time automatic bruise detection in (Apple) fruits using thermal camera. *Proceedings of the 2017 IEEE International Conference on Communication and Signal Processing, ICCSP 2017* 1080–1085. <https://doi.org/10.1109/ICCSP.2017.8286542>.
- Kuson, P., Terdwongworakul, A., 2013. Minimally-destructive evaluation of durian maturity based on electrical impedance measurement. *J. Food Eng.* 116, 50–56. <https://doi.org/10.1016/j.jfoodeng.2012.11.021>.
- Kuzy, J., Jiang, Y., Li, C., 2018. Blueberry bruise detection by pulsed thermographic imaging. *Postharvest Biol. Technol.* 136, 166–177. <https://doi.org/10.1016/j.postharvbio.2017.10.011>.
- Li, B., Lecourt, J., Bishop, G., 2018. Advances in non-destructive early assessment of fruit ripeness towards defining optimal time of harvest and yield prediction—a review. *Plants* 7, 1–20. <https://doi.org/10.3390/plants7010003>.
- Mangus, D.L., Sharda, A., Zhang, N., 2016. Development and evaluation of thermal infrared imaging system for high spatial and temporal resolution crop water stress monitoring of corn within a greenhouse. *Comput. Electron. Agric.* 121, 149–159. <https://doi.org/10.1016/j.compag.2015.12.007>.

- Mohd Ali, M., Hashim, N., Abd Aziz, S., Lasekan, O., 2020a. Exploring the chemical composition, emerging applications, potential uses, and health benefits of durian: a review. *Food Control* 113, 107189. <https://doi.org/10.1016/j.foodcont.2020.107189>.
- Mohd Ali, M., Hashim, N., Aziz, S.A., Lasekan, O., 2020b. Emerging non-destructive thermal imaging technique coupled with chemometrics on quality and safety inspection in food and agriculture. *Trends Food Sci. Technol.* 105, 176–185. <https://doi.org/10.1016/j.tifs.2020.09.003>.
- Munera, S., Amigo, J.M., Blasco, J., Cubero, S., Talens, P., Aleixos, N., 2017. Ripeness monitoring of two cultivars of nectarine using VIS-NIR hyperspectral reflectance imaging. *J. Food Eng.* 214, 29–39. <https://doi.org/10.1016/j.jfoodeng.2017.06.031>.
- Naik, S., Patel, B., 2017. Thermal imaging with fuzzy classifier for maturity and size based non-destructive mango (*Mangifera Indica* L.) grading. In: 2017 International Conference on Emerging Trends and Innovation in ICT, ICEI 2017. IEEE, pp. 15–20. <https://doi.org/10.1109/ETICT.2017.7977003>.
- Onsawai, P., Sirisomboon, P., 2015. Determination of dry matter and soluble solids of durian pulp using diffuse reflectance near infrared spectroscopy. *J. Near Infrared Spectrosc.* 23, 167–179. <https://doi.org/10.1255/jnirs.1158>.
- Pensiri, F., Visutsak, P., 2018. The watershed segmentation for durians classification. Proceedings of the 2018 International Conference on Image and Graphics Processing 83–87. <https://doi.org/10.1145/3191442.3191472>.
- Phuangsoambut, K., Phuangsoambut, A., Talabnark, A., Terdwongworakul, A., 2018. Empirical reduction of rind effect on rind and flesh absorbance for evaluation of durian maturity using near infrared spectroscopy. *Postharvest Biol. Technol.* 142, 55–59. <https://doi.org/10.1016/j.postharvbio.2018.04.004>.
- Raza, S.E.A., Prince, G., Clarkson, J.P., Rajpoot, N.M., 2015. Automatic detection of diseased tomato plants using thermal and stereo visible light images. *PLoS One* 10, 1–20. <https://doi.org/10.1371/journal.pone.0123262>.
- Siriphanich, J., 2011. Durian (*Durio Zibethinus* Merr.), Postharvest Biology and Technology of Tropical and Subtropical Fruits: Volume 3: Cocona to Mango. Woodhead Publishing Limited. <https://doi.org/10.1016/B978-1-84569-735-8.50005-X>.
- Somton, W., Pathaveerat, S., Terdwongworakul, A., 2015. Application of near infrared spectroscopy for indirect evaluation of “Monthong” durian maturity. *Int. J. Food Prop.* 18, 1155–1168. <https://doi.org/10.1080/10942912.2014.891609>.
- Sumriddetchkajorn, S., Intaravanne, Y., 2013. Two-dimensional fruit ripeness estimation using thermal imaging. ICPS 2013: International Conference on Photonics Solutions 1–6. <https://doi.org/10.1117/12.2019654>.
- Tagubase, J.Lou, Ueno, S., Yoshie, Y., Araki, T., 2016. Effect of freezing and thawing on the quality of durian (*Durio zibethinus murray*) pulp. *Trans. Japan Soc. Refrig. Air Cond. Eng.* 33, 1–6. https://doi.org/10.11322/tjsrae.16-17NR_OA.
- Tantisopharak, T., Moon, H., Youryon, P., Bunya-athichart, K., Krairiksh, M., Sarkar, T. K., 2016. Nondestructive determination of the maturity of the durian fruit in the frequency domain using the change in the natural frequency. *IEEE Trans. Antennas Propag.* 64, 1779–1787. <https://doi.org/10.1109/tap.2016.2533660>.
- Teh, B.T., Lim, K., Yong, C.H., Ng, C.C.Y., Rao, S.R., Rajasegaran, V., Lim, W.K., Ong, C. K., Chan, K., Cheng, V.K.Y., Soh, P.S., Swarup, S., Rozen, S.G., Nagarajan, N., Tan, P., 2017. The draft genome of tropical fruit durian (*Durio zibethinus*). *Nat. Genet.* 49, 1633–1641. <https://doi.org/10.1038/ng.3972>.
- Tifani, K.T., Nugroho, L.P.E., Purwanti, N., 2018. Physicochemical and sensorial properties of durian jam prepared from fresh and frozen pulp of various durian cultivars. *Int. Food Res. J.* 25, 826–834.
- Timkhum, P., Terdwongworakul, A., 2012. Non-destructive classification of durian maturity of “Monthong” cultivar by means of visible spectroscopy of the spine. *J. Food Eng.* 112, 263–267. <https://doi.org/10.1016/j.jfoodeng.2012.05.018>.
- Voon, Y.Y., Hamid, N.S.A., Rusul, G., Osman, A., Quek, S.Y., 2006. Physicochemical, microbial and sensory changes of minimally processed durian (*Durio zibethinus* cv. D24) during storage at 4 and 28 °C. *Postharvest Biol. Technol.* 42, 168–175. <https://doi.org/10.1016/j.postharvbio.2006.06.006>.
- Voon, Y.Y., Abdul Hamid, N.S., Rusul, G., Osman, A., Quek, S.Y., 2007. Characterisation of Malaysian durian (*Durio zibethinus* Murr.) cultivars: relationship of physicochemical and flavour properties with sensory properties. *Food Chem.* 103, 1217–1227. <https://doi.org/10.1016/j.foodchem.2006.10.038>.
- Wisutiamonkul, A., Promdang, S., Ketsa, S., Van Doorn, W.G., 2015. Carotenoids in durian fruit pulp during growth and postharvest ripening. *Food Chem.* 180, 301–305. <https://doi.org/10.1016/j.foodchem.2015.01.129>.
- Youryon, P., Rattanaphon, J., Supapvanich, S., Krairiksh, M., 2018. Physicochemical factors related to “Monthong” durian fruit maturity. *Acta Hort.* 1210, 165–169. <https://doi.org/10.17660/ActaHortic.2018.1210.23>.
- Zeng, X., Miao, Y., Ubaid, S., Gao, X., Zhuang, S., 2020. Detection and classification of bruises of pears based on thermal images. *Postharvest Biol. Technol.* 161, 111090. <https://doi.org/10.1016/j.postharvbio.2019.111090>.